ABSOLUTE INSTABILITY OF COMPRESSIBLE THREE-DIMENSIONAL FLOW

EWA TULISZKA-SZNITKO

Institute of Thermal Engineering,
Technical University of Poznan,
Piotrowo 3, 60-965 Poznan, Poland

Abstract: In the present paper the instability character (absolute/convective) of compressible viscous flow around geometries rotating in uniform flow is analysed. The linear local stability theory is used to investigate the boundary layer stability. Following the works of Briggs and Bers in the field of plasma physics, the absolute instability region is identified by singularities of dispersion relation called pinch — points. Calculations have been made for different Mach numbers and wall temperatures.

Keywords: numerical simulations, compressible flow, instabilities, absolute instability

1. Introduction

We analyse the instability character (absolute/convective) of compressible viscous flow around geometries rotating in uniform flow using linear local stability theory. The flow around rotating geometry is often used as a model problem because the boundary layer of rotating geometry is very similar to the boundary layer of swept wing flow. Both boundary layers are strongly three-dimensional and crossflow instability dominates. Lingwood [1], [2], [3] found regions of absolute instability in the incompressible boundary layer of disk rotating in still fluid. We have made calculations to find out whether absolutely unstable flow region exists in the compressible flow around a sharp cone of zero angle of attack rotating in uniform flow. We have also analysed the influence of physical parameters as Mach number, Reynolds number, crossflow Reynolds number and wall temperature on absolutely unstable regions.

The idea of the distinction between absolute and convective instability time was introduced for the first in the field of plasma physics by Briggs [4] and Bers [5]. The plasma physicists have made extensive contribution to the theoretical development of this idea. From a fluid mechanics point of view, this idea was considered in such survey articles as Monkewitz [6], Morkovin [7] and Huerre, Monkewitz [8].

In the local linear stability theory we used to choose either spatial or temporal theory. In spatial theory we assume that the wave number is complex and frequency

is real so the disturbances grow or decay with space and are periodic in time. In temporal theory we assume that disturbances grow or decay in time and are periodic in space. This implies that frequency is complex and the wave number is real. However, in real flow disturbances grow or decay in space and time. To find which type of analysis should be used it is necessary to determine the character of instability (absolute or convective). Spatial theory is irrelevant in absolutely unstable flow.

2. Absolute instability

To check the character of instability the flow is excited impulsively at a certain location in space and time. The response of the boundary layer shows whether the flow is absolutely or convectively unstable. Following the works of Briggs [4] and Bers [5] we define the flow as absolutely unstable if its impulse response grows with time at every location in space. In sufficiently large time a disturbance at a fixed point in space grows to an amplitude which can cause nonlinearity. As a result, in absolutely unstable flow any infinitesimal disturbance contaminates the entire flow field. If, by contrast, the impulse response decays at every location in sufficiently large time, the flow is convectively unstable. In convectively unstable flow the disturbance is swept away from the source as it grows. The waves travel far enough to reach sufficiently large amplitude to cause nonlinearity.

To determine the character of instability we use the linear local stability theory. In this theory the problem of obtaining distributions of disturbance amplitudes is reduced to solving an eigenvalue problem. The eigenfunctions exist only if wave number $k(\alpha, \beta)$ and frequency of waves ω satisfy a dispersion relation

$$D[k,\omega;\mathrm{Re}]=0, \tag{1}$$

where α and β are wave number components in streamwise ξ and spanwise η directions respectively (Figure 1).

According to the works of the Briggs [4] and Bers [5] the flow is absolutely unstable if its impulse response grows with time at every location in space. The response of a linear system to the forcing input can be determined by the Green function $G(x, t)$ (Huerre [8])

$$G(x,t)=\frac{1}{(2\pi)^2}\int_F\int_L \frac{e^{i(kx-\omega t)}}{D(k,\omega;\mathrm{Re})}d\omega dk, \tag{2}$$

where path F in the complex plane of wave number k is initially taken to be the real axis. The contour L in the complex frequency plane ω is chosen so that the causality is satisfied: $G(x, t) = 0$ everywhere when $t < 0$. In most cases the Fourier-Laplace integral (2) can not be evaluated for arbitrary chosen time, however, for a general dispersion relation one may obtain the time asymptotic Green function. From this asymptotic solution general mathematical criterion based on the properties of the dispersion relation (1) in complex k and ω planes has been derived to determine the nature of instability (Briggs [4]). According to

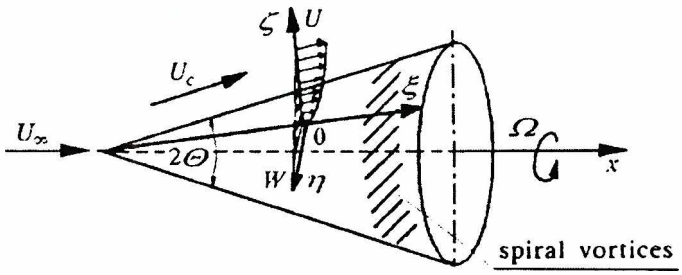

Figure 1. *Schematic picture of cone rotating in uniform flow*

this criterion the absolute instability can be identified by singularities in the dispersion relation called pinch — points. The pinch — points are located in a process of consecutive contour deformations in which L is deformed toward the lower half of ω plane (Kupfer [9]).

In Figure 2a curve $\omega(k)$ is obtained by mapping F contour along the real k axis into ω plane through the dispersion relation. If L is located above all singularities of dispersion relation (above curve $\omega(k)$ in Figure 2a) its image in the k plane i.e. spatial branches $k^+(\omega)$, $k^-(\omega)$, must lie in different halves of the k plane (lower and upper half). If one of these spatial branches crosses the original F contour, L itself would intersect the curve $\omega(k)$, which leads to a contradiction. Then, as L is displaced downward, both spatial branches move toward each other (Figure 2b).

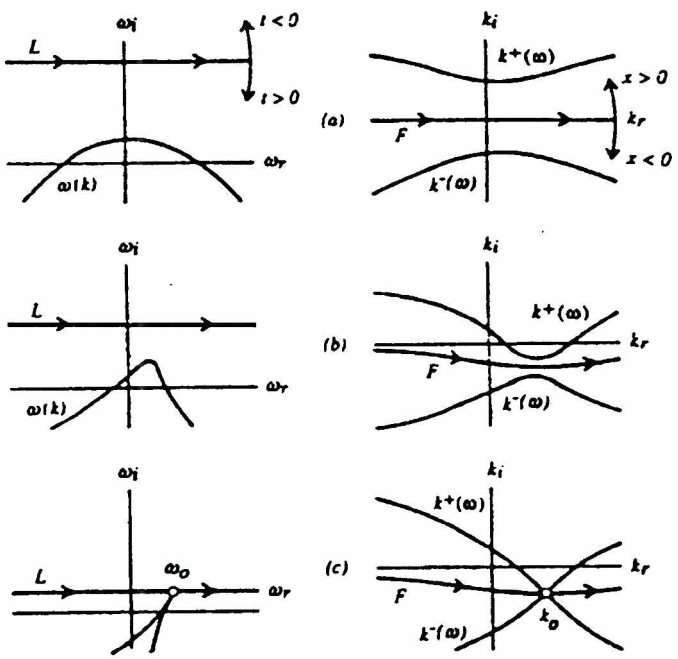

Figure 2. *Different stages of pinching process. Schematic picture of spatial $k^+(\omega)$, $k^-(\omega)$ and $\omega(k)$ temporal branches as L contour is displaced downward in complex ω plane.*

causality, the F contour must be deformed off the real k axis to avoid crossing. The process of deformation of F and L contours is finished when F is pinched by branches $k^+(\omega)$ and c. This point is indicated by k_o and ω_o. Pinch — points occur precisely where the group velocity is zero,

$$\frac{\partial \omega}{\partial k}(k_o) = 0. \tag{3}$$

We have the following criteria for absolute instability. The flow is absolutely unstable if so called absolute amplification rate ω_{oi} is positive ($\omega_{oi} > 0$). Additionally, for L contour located high enough in plane spatial branches $k^+(\omega)$ and $k^-(\omega)$ must lie in different halves of the k plane (Figure 2).

3. Governing equations

3.1 Perturbation equations

The linear local stability theory of compressible viscous flow is used to investigate the character of the instability of strongly three-dimensional boundary layer. Linear local stability equations are derived from the continuity equation, Navier-Stokes equations and energy equation of compressible gas.

In this research we formulate the compressible stability problem in a body-oriented coordinate system ξ, ζ, η shown in Figure 1 (ξ, ζ, η are coordinates in the streamwise, wall normal and spanwise directions respectively). All the lengths are scaled by the viscous scale $LS = \sqrt{\nu\xi / U_e}$ and all physical parameters by the corresponding boundary layer edge value. Reynolds number is defined in the following manner:

$$\mathrm{Re} = \sqrt{U_e \xi / \nu_e}. \tag{4}$$

Perturbation equations are obtained by decomposing all parameters into the steady basic flow and the unsteady disturbance flow component. Linear local stability equations of compressible parallel flow are reduced to ordinary differential equations:

$$(AD^2 + BD + C)\Psi = 0, \tag{5}$$

where A, B, C are 5×5 matrices and $\Psi = [\bar{u}, \bar{v}, \bar{w}, \bar{\tau}, \bar{p}]^T$ ($\bar{u}, \bar{v}, \bar{w}$ are amplitude of velocity components in ξ, ζ, η directions, $\bar{\tau}$ is amplitude of temperature and $\bar{p}$ is amplitude of pressure). We have the following homogeneous boundary conditions at the wall and in the infinity for the velocity components and temperature amplitude functions:

$$\bar{u}(0)=\bar{v}(0)=\bar{w}(0)=\bar{\tau}(0)=0,$$
$$\bar{u}(\bar{\zeta})=\bar{v}(\bar{\zeta})=\bar{w}(\bar{\zeta})=\bar{\tau}(\bar{\zeta})=0, \qquad \bar{\zeta}\to\infty\ . \tag{6}$$

Linear stability equations (5) are solved using the fourth order accurate two point scheme which is derived by means of the Euler-Maclaurin formula (Malik [10], Balacumar [11], Tuliszka-Sznitko [12]).

$$\varphi^{k}-\varphi^{k-1}=\left(\frac{h_k}{2}\right)\left[\frac{d\varphi^{k}}{d\bar{\zeta}}+\frac{d\varphi^{k-1}}{\partial\bar{\zeta}}\right]-\left(\frac{h_k^2}{12}\right)\left[\frac{d^2\varphi^{k}}{\partial\bar{\zeta}^2}-\frac{d^2\varphi^{k-1}}{d\bar{\zeta}^2}\right]+0\left(h_k{}^5\right), \tag{7}$$

where $\varphi^k=\varphi(\bar{\zeta}_k)$, $h_k=\bar{\zeta}_k-\bar{\zeta}_{k-1}$, $\bar{\zeta}=\zeta/LS$. To apply scheme (7) to equations (5) we formulate them as a set of first order differential equations:

$$\frac{d\varphi_n}{d\bar{\zeta}}=\sum_{m}^{8}a_{nm}\varphi_m, \qquad n=1...8, \tag{8}$$

where:

$$\varphi_1=\bar{u},\quad \varphi_2=d\bar{u}/d\bar{\zeta},\quad \varphi_3=\bar{v},\quad \varphi_4=\bar{p},\quad \varphi_5=\bar{\tau},$$
$$\varphi_6=d\bar{\tau}/d\bar{\zeta},\quad \varphi_7=\bar{w},\quad \varphi_8=d\bar{w}/d\bar{\zeta}.$$

Final algebraic system of equations with the boundary conditions can be written in the following form

$$A_k\varphi^{k-1}+B_k\varphi^{k}+C_k\,\varphi^{k+1}=H_k, \tag{9}$$

where A_k, B_k, C_k are 8×8 matrices and H is a 8×1 null matrix. The eigenvalue problem is solved directly. Block elimination method is used to solve algebraic system of equations.

3.2 Basic state

The basic state is obtained from boundary equations of rotating cone (Illingworth [13]) using Mangler transformation

$$x=\frac{1}{L^2}\int_0^{\xi}r^2(\xi)d\xi, \qquad y=\frac{r(\xi)\zeta}{L} \tag{10}$$

and similarity solutions (Koh, Price, [14], Illingworth [13]):

$$\Psi(x,y)=\sqrt{\rho_e\mu_e U_e x}\,f(x,s), \qquad ds=\sqrt{\frac{U_e\rho_e}{\mu_e x}}\rho dy, \tag{11}$$

where L is a reference length taken in as a unity for computations. After transformations the system of rotating cone boundary layer equations can be written in the following form:

$$\frac{x}{\rho}\frac{dU_e}{dx}+\frac{\partial}{\partial s}\left(\mu\rho\frac{\partial^2 f}{\partial s^2}\right)+\frac{1}{2}f\frac{\partial^2 f}{\partial s^2}\left[1+x\frac{1}{U_e}\frac{dU_e}{dx}\right]+\frac{WW}{3}=$$

$$x\left[\frac{\partial f}{\partial s}\frac{\partial^2 f}{\partial x\partial s}-\frac{\partial f}{\partial x}\frac{\partial^2 f}{\partial s^2}+\frac{1}{U_e}\frac{dU_e}{dx}\left(\frac{\partial f}{\partial s}\right)^2\right],$$

$$\frac{\partial}{\partial s}\left(\mu\rho\frac{\partial W}{\partial s}\right)+\frac{1}{2}f\frac{\partial W}{\partial s}\left[1+x\frac{1}{U_e}\frac{dU_e}{dx}\right]-\frac{1}{3}W\frac{\partial f}{\partial s}=x\left[\frac{\partial f}{\partial s}\frac{\partial W}{\partial x}-\frac{\partial f}{\partial x}\frac{\partial W}{\partial s}\right], \tag{12}$$

$$\frac{\partial}{\partial s}\left(\mu\rho\frac{\partial h}{\partial s}\right)+\frac{\mathrm{Pr}}{2}f\frac{\partial h}{\partial s}\left[1+x\frac{1}{U_e}\frac{dU_e}{dx}\right]+\mathrm{Pr}\rho\mu Ma_e^2\left[\left(\frac{\partial^2 f}{\partial s^2}\right)^2-\left(\frac{\partial W}{\partial s}\right)^2\right]=$$

$$x\mathrm{Pr}\left[\frac{\partial f}{\partial s}\frac{\partial h}{\partial x}-\frac{\partial f}{\partial x}\frac{\partial h}{\partial s}\right]+\mathrm{Pr}\frac{x}{\rho}Ma_e^2\frac{1}{U_e}\frac{dU_e}{dx}\frac{\partial f}{\partial s},$$

$$\rho h=1,$$

where h is the dimensionless enthalpy and Pr is Prandtl number. All physical parameters are scaled by the corresponding boundary layer edge value. The boundary conditions are:

$$f=\frac{\partial f}{\partial s}=0,\quad W=\frac{\Omega}{U_e}\sqrt{3x\sin\Theta},\quad \begin{cases}(i)\dfrac{\partial h}{\partial s}\\ (ii)h=const\end{cases}\quad s=0 \tag{13}$$

$$\frac{\partial f}{\partial s}=1,\qquad W=0,\qquad h=1\qquad s\to\infty.$$

The final partial differential equations are solved using Keller Box method. The inviscid flow velocity U_e is proportional to ξ^m. The parameter m depends solely on the cone angle (Koh, Price [14]).

4. Results

To find the regions of absolute instability, we apply Briggs [4] criterion with fixed wave number component in spanwise direction β. Calculations are made for small half angles of the cone Θ = 0.5 – 7.5° to make the approximation error of parallel flow model negligible.

In Figure 3 the development of two spatial branches $\alpha^+(\omega)$, $\alpha^-(\omega)$ in the

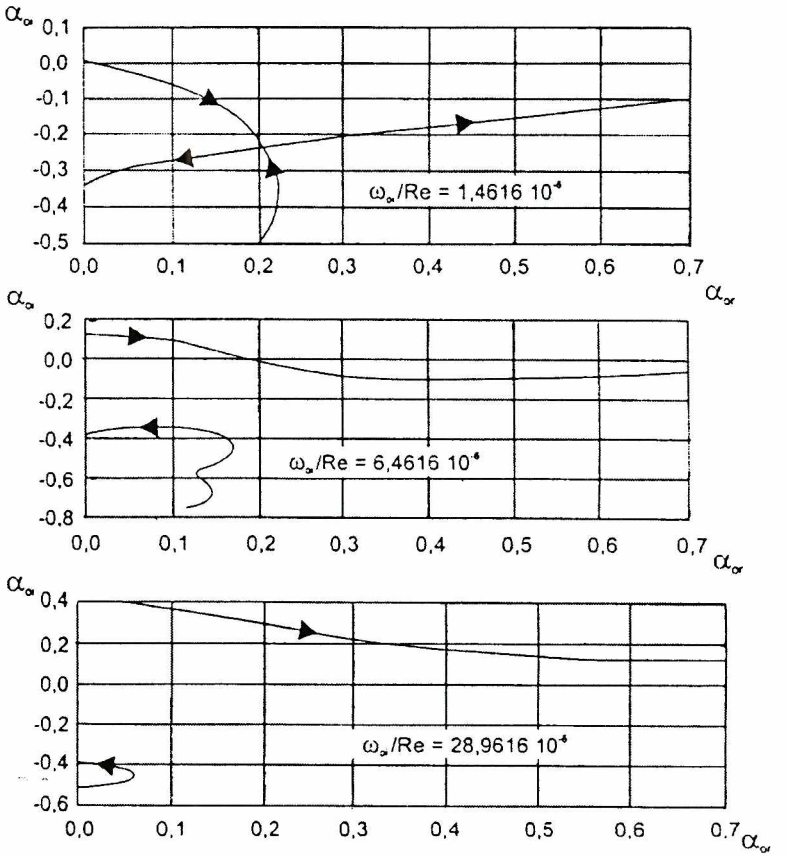

Figure 3. *Development of special branches obtained for different ω_i/Re: ω_i/Re = 1.4616E-06, 6.4616E-06, 28.9616E-06, Re = 5560, Ma_e = 0.2, Θ = 4.0°, Ω/U_e = 19.5, β = 0.216, adiabatic wall.*

complex α plane is shown. Results are obtained for half angle of the cone $\Theta = 4.0°$, edge Mach number $Ma_e = 0.2$, Reynolds number Re = 5560, dimensionless rotational speed $\Omega/U_e = 19.5$, component of wave number in spanwise direction $\beta = 0.216$ and for values of ω_i/Re = 1.4616E-06 (a), 6.4616E-06 (b) and 28.9616E-06 (c). The arrows in Figure 3 indicate the direction of increasing frequency ω_r. In Figure 4 we have a temporal branch $\omega(\alpha)$ obtained for horizontal line in α plane ($\alpha_i = -0.24066$). The tip of this cusp like form indicates the pinch — point in ω plane. We have found the pinch — point at $\alpha_o = (0.20412, -0.24066)$ and ω_o/Re = (134.47E-06, 1.4616E-06). Absolute amplification rate at this point is positive and for sufficiently large ω_i the spatial branches $\alpha^+(\omega)$, $\alpha^-(\omega)$ lie in different halves of α–plane so at this point the flow is absolutely unstable.

In Figure 5 the variations of ω_{oi}/Re versus β are analysed. Calculations are made for $Ma_\infty = 0.35$, $\Theta = 7.5°$, $\Omega/U_e = 12.0$ and for different Reynolds numbers Re = 5760, 5000, 4700. The points at which curves ω_{oi}/Re = $f(\beta)$ in Figure 5 cross the real axis limit the absolutely unstable regions.

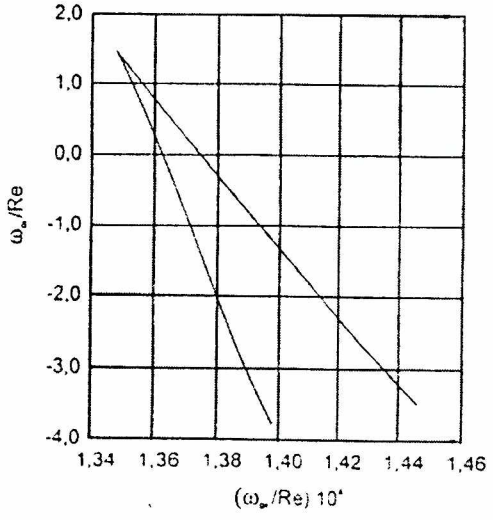

Figure 4. *Result of mapping of contour $\alpha_i = -0.24066$ from α plane to ω plane; Re = 5560, $Ma_e = 0.21$, $\Theta = 4.0°$, $\Omega \times 1/U_e = 19.5$, $\beta = 0.216$, adiabatic wall.*

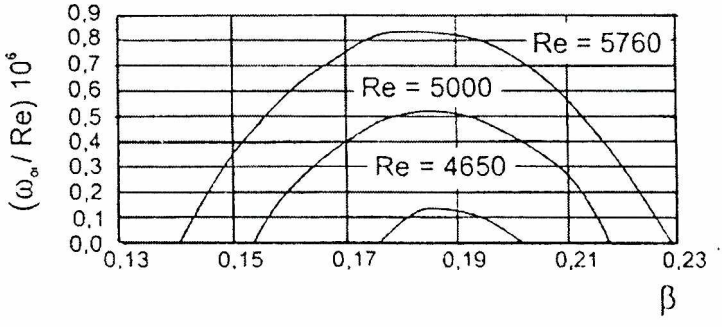

Figure 5. *Variations of ω_{or}/Re and ω_{oi}/Re versus β; Re = 5760, 5000, 4700, $Ma_\infty = 0.35$, $\Theta = 7.5°$, $\Omega/U_e = 12.0$, adiabatic wall.*

Figure 6a and b show the neutral absolute stability curves obtained in (α_{oi}, Re) and (α_{or}, Re) planes respectively. Calculations are made for $\Theta = 7.5°$, $\Omega/U_e = 12.0$ and for $Ma_\infty = 0.35$, 0.4. Inside these curves absolute amplification rates ω_{oi} are positive and outside the curves they are negative; consequently inside we have the absolutely unstable regions and outside the convectively unstable regions. We see that absolutely unstable region of the flow decreases with increasing Mach number. Figure 7 shows critical Reynolds numbers of the neutral absolute instability curves Re_{CRabs} versus Mach numbers Ma_∞ and β (calculations are made for $\Theta = 7.5°$ and $\Omega/U_e = 12.0$). Critical Reynolds number increases very rapidly with increasing Mach number. Cusp like forms obtained for $Ma_e = 0.218$, $Ma_e = 0.423$, $Ma_e = 0.529$ and $Ma_e = 0.636$ are shown in Figure 8 (Re = 5760, $\Theta = 7.5°$, $\Omega/U_e = 12.0$,

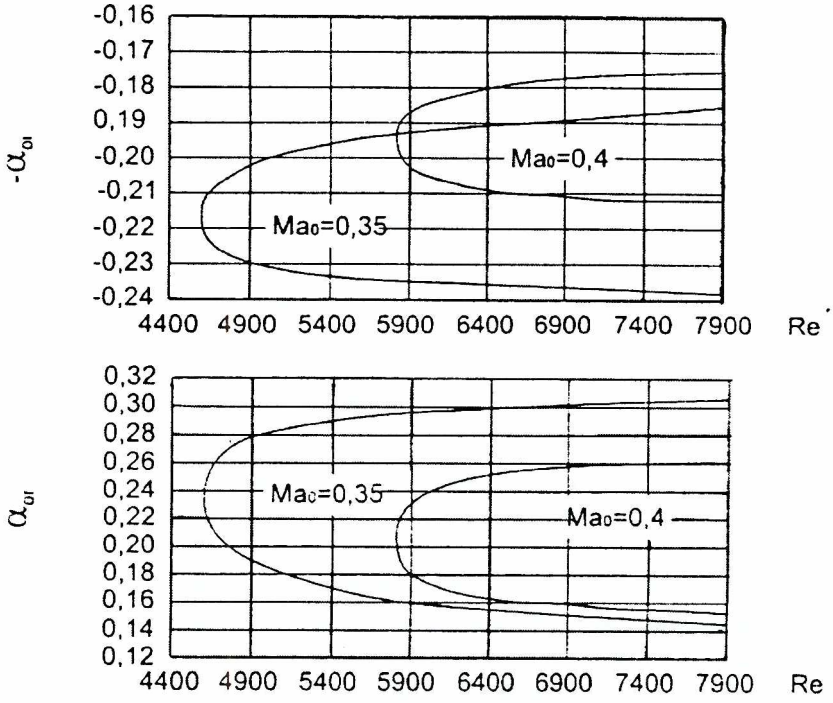

Figure 6. *Absolutely unstable neutral curves. $Ma_\infty = 0.35, 0.4$, $\Theta = 7.5°$, and $\Omega/U_e = 12.0$, adiabatic wall.*

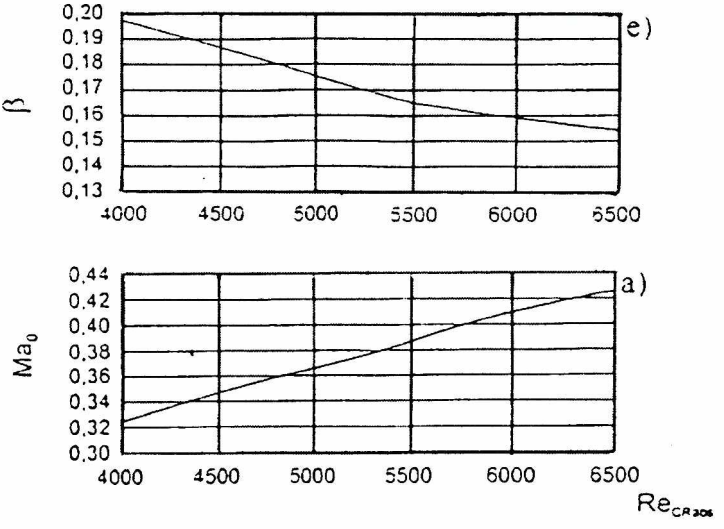

Figure 7. *Mach numbers Ma_∞ and β versus critical Reynolds numbers of the neutral absolute instability curves Re_{CRabs} ($\Theta = 7.5°$, $\Omega/U_e = 12.0$).*

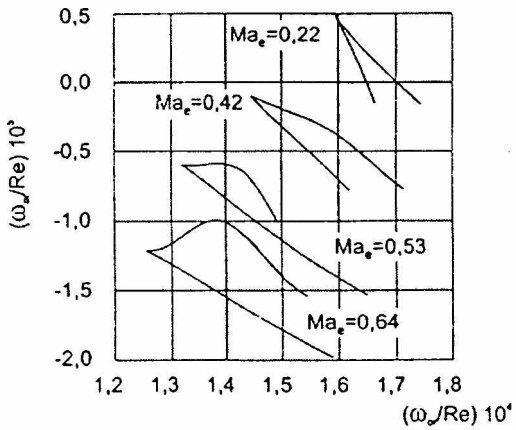

Figure 8. *Cusp like forms obtained for Mach number Ma_e = 0.218, 0.423, 0.529 and 0.636; Re = 5760, $\Theta = 7.5°$, Ω/U_e = 12.0, β = 0.216, adiabatic wall.*

$\beta = 0.216$). Again we observe the same influence of increasing Mach number; absolute amplification rates in Figure 8 decrease with increasing edge Mach number. To obtain positive absolute amplification rates for higher edge Mach numbers it is necessary to increase rotational speed of the cone i.e. it is necessary to increase crossflow Reynolds number. We did not find absolutely unstable regions in supersonic flows around rotating cone.

The region of absolutely unstable flow decreases with decreasing wall temperature. In Figure 9 the variations of the absolute amplification rate versus β and different temperature rate T_w / T_{ad} are shown (w and ad denote the wall and adiabatic temperatures, respectively). Calculations are obtained for $\Theta = 4.0°$, $Ma_e = 0.2$, Re = 5560 and $\Omega/U_e = 19.5$. In Figure 10 there are cusp like forms

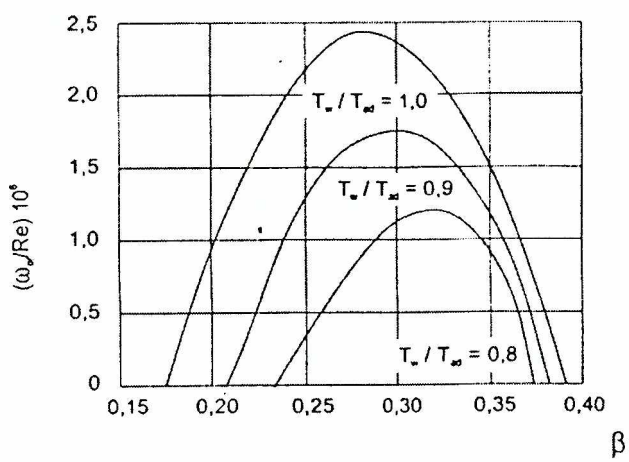

Figure 9. *Variations of location of pinch — points versus β and temperature rates T_w / T_{ad}. Re = 5560, $\Theta = 4.0°$, Ma_e = 0.2 and Ω/U_e = 19.5.*

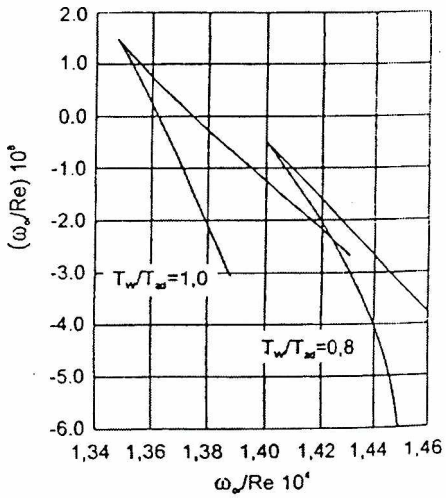

Figure 10. *Cusp like forms obtained for wall temperature rates T_w / T_{ad} = 1.0 and 0.8; $Re = 5560, \Theta = 4.0°$, $Ma_e = 0.2$ and $\Omega/U_e = 19.5$, $\beta = 0.216$.*

obtained for the same parameters but for different wall temperatures $T_w / T_{ad} = 1.0$ and 0.8. The absolute amplification rate is smaller for lower wall temperature.

5. Conclusions

In this paper we analyse the character of instability of the flow around a cone of zero angle of attack rotating in uniform flow. We considered the cone of small half angle. This model problem allowed us to investigate the influence of such physical parameters as wall temperature and edge Mach number on absolutely unstable flow regions using linear local stability theory. Convective instability of the flow around cone rotating in uniform flow was considered in previous works (Tuliszka-Sznitko [12], [15], [16]).

We found that boundary layer of cone rotating in uniform flow can be absolutely unstable over a range of β. We presented the neutral stability curves for different Mach number, which showed absolutely unstable regions. We found that the absolute amplification rate decreased with increasing edge Mach number and decreased with decreasing wall temperature. We did not find absolutely unstable regions in supersonic flows.

Parallel flow approximation used in linear stability theory can have small influence on results but the influence of physical parameters on absolutely unstable regions and the general instability characteristics obtained in this paper are still relevant.

Acknowledgement

The author is very grateful to Prof. Walter Riess from the University of Hannover for help and cooperation.

References

[1] Lingwood R., *Absolute instability of the boundary layer on a rotating disk*, J. Fluid. Mech., vol. 299, 1995, pp. 17–33

[2] Lingwood R., *An experimental study of absolute instability of the rotating- disk boundary layer flow*, Fluid. Mech., vol. 314, 1996, pp. 373–405

[3] Lingwood R., *Absolute instability of the Ekman layer and related rotating flows*, J. Fluid. Mech., no. 331, 1997, pp. 405–428

[4] Briggs R., *Electron-Stream Interaction with Plasmas*, MIT Press, 1964

[5] Bers, A., *Linear waves and instabilities, In Physique des Plasmas* (ed. C. DeWitt and J. Peyraud), Gordon & Breach, 1975, pp. 117–215

[6] Monkewitz P., *The role of absolute and convective instability in predicting the behaviour of fluid system*, Proc. ASME Fluids Eng. Spring Conf. La Jolla, Calif, 1989

[7] Morkovin M., *Recent insights into instability and transition to turbulence in open flow system*, AIAA Pap., no. 88-3675, 1988

[8] Huerre P., Monkewitz P., *Local and global instabilities in spatially developing flows*, Annu. Rev. Fluid. Mech., vol. 22, 1990, pp. 473–537

[9] Kupfer K., Bers A., Ram A., *The cusp map in the complex - frequency plane for absolute instabilities*, Phys. Fluids, no. 30, 1987, pp. 3075–3082

[10] Malik M., Chuang S., Hussaini M., *Accurate numerical solution of compressible linear stability equations*, ZAMP, no. 33, 1982, pp. 189–201

[11] Balacumar P., Reed H., *Stability of three dimensional boundary layers*, Report of Department of Mechanical and Aerospace Engineering, Arizona State University, 1989

[12] Tuliszka-Sznitko E., *Niestabilność trójwymiarowej warstwy przyściennej*, WPP seria Rozprawy, no. 287, 1993

[13] Illingworth C., *The laminar boundary layer of rotating body of revolution*, Philosophical Magazine, vol. 44, 1953, pp. 473–537

[14] Koh J., Price J., *Nonsimilar boundary layer heat transfer of a rotating cone in forced flow*, Transaction of ASME, Journal of Heat Transfer, 1967, pp. 139–145

[15] Tuliszka-Sznitko E., *Instability of non-parallel compressible boundary layer*, MTiS, Fluid Mechanics, no. 2, vol. 35, 1996, pp. 447–463

[16] Tuliszka-Sznitko E., *Instability of boundary layer on rotating geometries, Numerical Methods in Laminar and Turbulent Flow*, vol. 10, Pineridge Press, Swansea U.K., 1997, pp. 1061–1072